THERMOPHYSICAL CHARACTERIZATION OF TERRESTRIAL ANALOGS FOR MARTIAN SEDIMENTARY FEATURES. J. E. Moersch,[1] S. C. Whisner[1], and C. Hardgrove[1], [1]Department of Earth and Planetary Sciences, University of Tennessee, 1412 Circle Dr., Knoxville, TN 37996, USA, jmoersch@utk.edu

Introduction: One of the most interesting results to come out of the past four years of remote sensing data analysis from orbiting spacecraft at Mars has been the identification of small-scale constructional sedimentary features related to flowing or standing liquid water on the surface. Features interpreted to be deltas [e.g., 1-5] and alluvial fans [e.g., 6-9] have been identified in high-resolution visible images of the surface, suggesting both sustained and episodic fluvial processes. Earlier work [10] also suggested the presence of evaporite deposits in concentric rings along the margins of possible Martian paleolakes.

The aforementioned studies relied primarily on photogeologic and geomorphic analyses of imaging and topographic data, along with comparisons to terrestrial examples. Surprisingly little use has been made of thermal imaging observations. Thermal images from the Thermal Emission Imaging System (THEMIS) may be used to make maps of the thermal inertias on the Martian surface [e.g., 11]. Thermal inertia is primarily a function of the sizes of particles making up the surface and the surface's degree of induration. Sedimentary processes that create deltas and alluvial fans spatially sort particles by their grain sizes. Evaporating lakes precipitate different species of salts, cemented to varying degrees, in characteristic spatial patterns. Thus, we suggest that orbital thermal images may help confirm or refute identifications of Martian deltas, alluvial fans, and paleolakes through the presence or absence of characteristic spatial patterns in thermal inertias that result from particle size distributions and patterns of cementation.

Before a full assessment of thermal inertia patterns on Martian sedimentary features is made, it is useful to understand how these patterns manifest themselves on terrestrial examples of similar features. Terrestrial analogs offer the advantage of easy access for ground-truthing particle size distributions, soil induration, and other factors contributing to thermal inertia.

We have recently begun a three-year study funded by NASA's Mars Fundamental Research Program to characterize distributions of thermal inertias on an assortment of terrestrial deltas, alluvial fans, and evaporite deposits. Our objective is to look for spatial patterns in thermal inertias that are characteristic, if not diagnostic, of these features and their subclasses (e.g., fluvial-dominated vs. debris flow-dominated alluvial fans). We are also studying the thermal behavior of terrestrial sand dunes as a control subject to isolate geometric effects on apparent thermal inertias. Ultimately, we hope to apply our understanding of thermal inertia patterns in terrestrial sedimentary features to evaluate their Martian counterparts.

Here we report on our analyses of our first set of targets, two sand dune fields in California and a man-made model dune. These targets were chosen to help understand the effects of slope and slope orientation on apparent thermal inertias. We also present preliminary data from our first observations of alluvial fans.

Method: Our primary tool for characterizing spatial patterns of thermal inertias on terrestrial sedimentary features is a 320x240 pixel, broadband thermal infrared camera manufactured by FLIR Systems (Model S45). High-resolution images from our camera are complemented by day/night thermal infrared images acquired by the Advanced Spaceborne Thermal Emission and Reflection Radiometer (ASTER) instrument on the EOS-Terra satellite [12]. This instrument provides comparable spatial resolution (90m/pixel) to that of THEMIS at Mars.

We observe targets with our camera in two modes: Individual images of targets are acquired at key times of day (e.g., pre-dawn) from a light aircraft to give an overhead perspective similar to that seen from orbit, but at higher spatial resolution. In the other mode of observation, time-lapse images are obtained by mounting the camera to a tripod on the ground. Images taken in this mode are acquired several times per hour over the course of at least one diurnal cycle. Concurrent meteorological observations (air temperature, humidity, barometric pressure) are made with a Nielson-Kellerman Kestrel 4000 pocket weather station. Images from the time-lapse sequence are stacked into a single data product called a hypertemporal image cube, in which two dimensions are the spatial dimensions of the scene and the third dimension is time of day. Temperature values extracted for a single spatial pixel along the time axis of this image cube comprise a diurnal thermal curve for that pixel's location.

Quantitative models for extracting thermal inertias from Martian thermal data are not appropriate for use on terrestrial subjects because of the Earth's thicker atmosphere. Rather, terrestrial subjects have typically been evaluated in terms of relative thermal inertias that are comparable to each other within a given scene. The most common approach is the Apparent Thermal Inertia (ATI) model [13,14]. The ATI value of a pixel is given by simply dividing the co-albedo ($1 - A$) of

the pixel by the change in temperature (ΔT) of the pixel from the coldest to the warmest times of the day. More recently, an approach called Differential Apparent Thermal Inertia (DATI) has been advocated [15]. In this method, thermal inertia is approximated by measuring the rate of heating (dT/dt) of a surface over a short period (20-120 minutes) in either the morning or evening hours. We use both the ATI and DATI methods (as well as simple visual inspection of diurnal thermal curves) to evaluate our thermal image data. Part of our study is a critical evaluation of these models for characterizing thermal inertias of non-horizontal surfaces.

Our remote observations are supported by extensive ground-truthing measurements on the targets. Within a given scene, we select about a dozen or more stations for ground-truth measurements. Stations are chosen to represent the range of different surface types and surface orientations present on the target. At each station, we measure slope and slope orientation with a Brunton compass, and albedo with an ALTA II handheld reflectance spectrometer. Particle size distributions are characterized either by collecting samples (for fine-grained components) and sieving them in the laboratory or (for larger-grained surfaces) setting up a measurement grid on the surface and collecting digital images for clast diameter measurements. Soil samples are collected in sealed containers for measurements of moisture content in the lab. For future targets, where soil induration may be a factor, a cone penetrometer will be used to characterize induration. All of the ground-truthing measurements from each station in the scene are treated as independent variables that are examined for correlations with the diurnal thermal curve from the appropriate pixels in the remote sensing observations.

Sand dune observations: Particle size and degree of induration are the two primary compositional controls on thermal inertia, but geometric factors such as surface slope and slope orientation can also affect the apparent thermal inertia of a surface because of differences in diurnal insolation histories – so-called "thermoclinometric effects." As a first step in our project, we have collected a set of thermal image observations of terrestrial sand dunes and a man-made model dune. Dunes have relatively unimodal particle size distributions and uniform albedos, but their slopes and slope orientations can vary significantly. Diurnal thermal imaging sequences of dunes help us to isolate the effects of slope geometry on apparent thermal inertias. The understanding of geometric effects thus gained will help in subsequent analyses of other types of sedimentary features, which feature combinations of geometric and compositional variations.

The subjects for the dune portion of our study were the Dumont Dunes in California's Mojave Desert, the Eureka Dunes in Death Valley National Park, California, and a man-made model dune constructed outside on a building rooftop at the University of Tennessee. The two dune fields provided the advantage of being natural features observed at similar ranges as the other sedimentary features in our study, but carried the disadvantage of only displaying a limited range of slope azimuths when viewed from a single camera vantage point. The man-made dune was small enough to allow observation of 360 degrees of slope azimuths in a single camera scene.

The model dune consisted of a pile of sand approximately 1m in diameter, uniform in grain size and albedo. The sides of the model dune were shaped into twelve flat facets oriented in 30 degree increments around the azimuth angles of the compass. The slope of each facet was near the angle of repose. The size of the model was chosen to be large enough that the temperatures at the centers of each facet would not be significantly influenced by the presence of other facets or the underlying ground. The thermal camera was perched above the model dune in such a way that all twelve facets could be observed in a single camera scene.

Figure 1 shows an example thermal image plane from the Dumont Dune hypertemporal image cube. Figure 2 shows three example diurnal curves extracted from this image cube from three different faces of the dunes, oriented at approximately 90 degree azimuth intervals. Differences in the diurnal curves are immediately apparent. Although all three dune faces start out at approximately the same temperature in the predawn hours, the maximum temperatures reached are significantly different (ΔT varies by more than a factor of two). There are also differences in the morning heating rates (dT/dt) and in the amount of time required for each face to reach its maximum temperature (Δt).

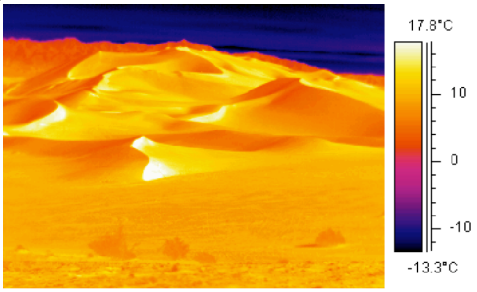

Figure 1: Thermal infrared image of Dumont Dunes, looking east.

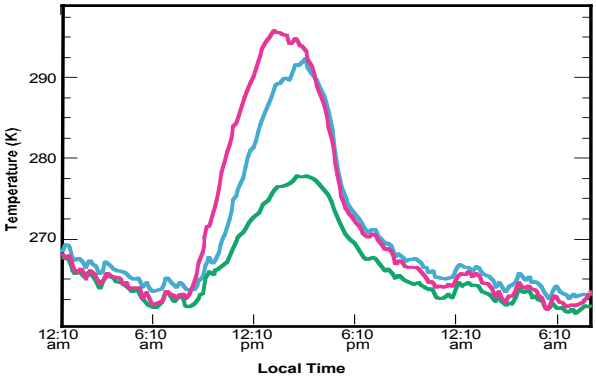

Figure 2: Three example diurnal curves from three different dune faces observed in the Dumont Dunes hypertemporal image cube. Purple curve is approximately south-facing, cyan curve is approximately west-facing, and green curve is approximately north-facing.

The same types of differences observed in the three example diurnal curves plotted in Figure 2 are found in all of our sand dune data. Figure 3 shows plots of the aforementioned parameters - ΔT, morning heating rates (dT/dt), and time between pre-dawn minimum temperature and the maximum temperature (Δt) – for all of our dune measurements, plotted as a function of slope azimuth. The slope orientation data and corresponding parameters for the diurnal curves are compiled from the positions of eleven ground-truth stations at Dumont Dunes, thirteen ground-truth stations at Eureka Dunes, and the twelve faces of our model dune.

The fact that the three sets of dune observations are vertically offset from one another on the parameter plots in Figure 3 is not significant – this simply reflects the fact that there were different ambient temperatures on the days of the different observations or differences in albedo between the three dunes. The fact that the observations were taken in different months and at different latitudes (leading to different solar elevations and lengths of days) may also contribute to the offsets. The significant point illustrated in Figure 3 is that all three sets of dune observations appear to follow similar trends: the three parameters chosen to characterize differences in the diurnal temperature curves are strongly correlated with slope azimuth angle.

This result is significant because the parameters plotted in Figure 3 would normally be associated with differences in the thermal inertia of the surfaces – assuming constant albedo, ΔT would be inversely correlated with ATI, dT/dt would be inversely correlated with DATI, and Δt would be directly correlated with a simple, intuitive concept of thermal inertia (high thermal inertia surfaces take longer to heat up). Our

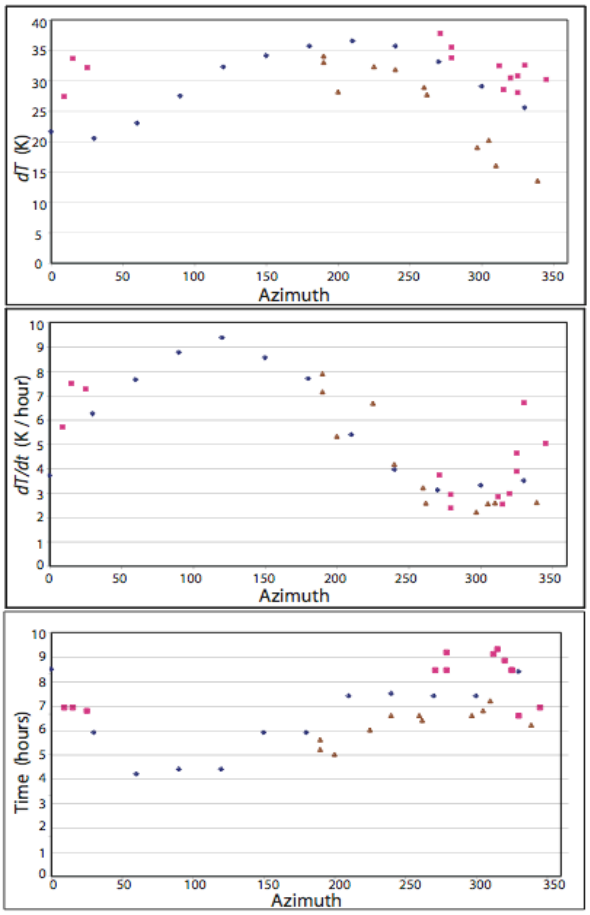

Figure 3: Measured parameters extracted from diurnal thermal curves from multiple facets on all three dune targets (Eureka dunes in blue dimonds, Dumont Dunes in orange triangles, and the model dune in pink squares): a) Difference between maximum and minimum temperature (ΔT) as a function of slope azimuth; b) Morning heating rate (dT/dt) between 7:30 am and 9:30 local time; c) Time between minimum and maximum temperature (Δt) in the morning.

ground truthing measurements indicated that each set of dunes had nearly uniform albedos and statistically indistinguishable particle size distributions – the latter implying that the actual thermal inertias for each dune were uniform. The fact that the three parameters plotted in Figure 3 are not constant with azimuth angle for each dune indicates that the standard methods for characterizing terrestrial thermal inertias should not be used when dealing with non-horizontal targets. Thermoclinometric slope azimuth effects can "spoof" techniques such as ATI or DATI into seeing apparent thermal inertia variations that bear no relation to the physical characteristics of the material on the ground.

Alluvial fan observations: Thus far, we have acquired preliminary ground-based thermal observations

of two terrestrial alluvial fans, one near Badwater in Death Valley, and another adjacent to the dunes in Eureka Valley. Figure 4 shows an example image from the hypertemporal image cube taken at Badwater, with representative diurnal thermal curves taken from four locations in the scene. Although these diurnal curves have not been corrected for slope orientation or range to the camera, initial inspection confirms that the general trends expected for spatial patterns on alluvial fans are present. The diurnal curve taken from the apex of the fan has the smallest ΔT, while other points further down the fan have progressively larger ΔTs. This trend in ΔT is consistent with higher thermal inertia materials being located at the top of the fan, grading to smaller particle sizes toward the toe of the fan, a pattern broadly consistent with what would be expected from the sedimentological sorting processes that formed the fan.

One advantage to the hypertemporal image cube data product is that it may be subjected to the same types of data analysis techniques that are usually applied to hyper*spectral* cubes to map compositions. Figure 5 shows a single band that was created from a principle component transformation of the hypertemporal cube in Figure 5. Theoretically, this type of manipulation should segregate different factors contributing to variability in the diurnal curves into different output bands. The band shown in Figure 6 appears to be sensitive to thermal inertia variations. Trends in brightness can be seen between the head and toe of the fan, and a hint of a surface distributary network (perhaps channels filled with fine grains) is visible radiating away from the apex down the fan. Future ground-truthing will be necessary to verify this interpretation.

Future work: Our current work on sand dunes will conclude shortly with a set of aerial thermal images to complement the ground-based work already-carried out. We will attempt to use the dune data to develop a modification to the ATI and/or DATI techniques for modeling terrestrial thermal inertias that above. Next, we will begin our focused campaign on compensates for the slope orientation effects described alluvial fans, making ground and aerial-based observations of a variety of fan types, looking for similarities and differences in the spatial patterns of thermal inertias they display. In subsequent years of the project, we will turn our attention to terrestrial deltas and evaporite deposits.

References: [1] Pondrelli, M. et al. (2005) *JGR, 110*, E04016. [2] Bhattacharya, J.P. et al. (2005) *GRL, 32*, L10201. [3] Mangold, N. and Ansan, V. (2006) *Icarus, 180*, 75-87. [4] Lewis, K. and Aharonson, O. (2006) *JGR, 111,* E06001. [5] Weitz et al. (2006) *Icarus, 184,* 436-451. [6] Pondrelli, M., et al. (2004) LPS XXXV, [7] Moore, J.M., and Howard, A.D., (2005) *JGR, 110,* E04005. [8] Howard, A.D., et al. (2005) *JGR, 110,* E12S14. [9] Di Achille, G., et al. (2006) *GRL, 33,* L07204. [10] Cabrol and Grin (1999), *Icarus, 142*, 160-172. [11] Fergason, R.L., et al. (2006) *JGR, 111,* E12004. [12] Abrams, M. (2000) *Int'l J. Remote Sensing, 21,* 847-859. [13] Price, C. (1977) *JGR, 82,* 2582-2590. [14] Gupta, R.P. (2003) Remote Sensing Geology, 199, and refs therein. [15] Sabol, D., et al. (2006) *Int'l Symp. on Recent Adv. in Quant. Rem. Sens.*

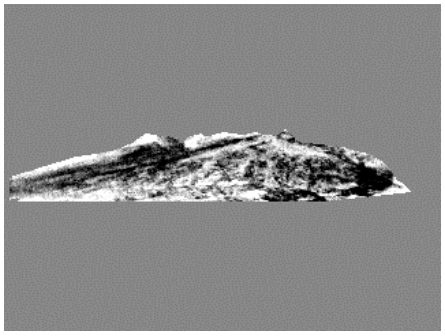

Figure 6: A principle component (PC) band from the hypertemporal cube shown in Figure 5. Pixels not on the fan were masked for the PC transformation.

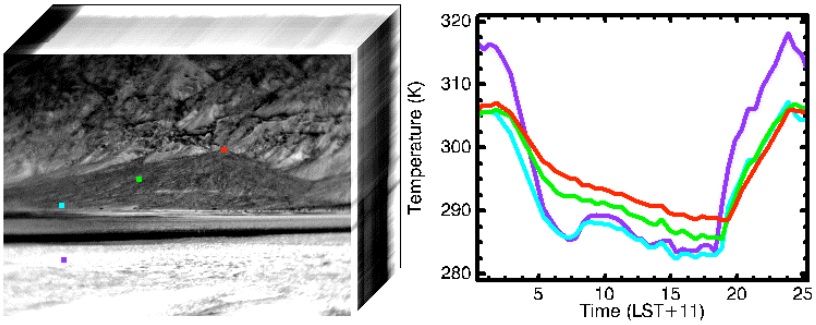

Figure 5: A thermal image from a hypertemporal image cube of a debris-flow dominated alluvial fan (left), with associated diurnal temperature curves for selected locations (right). Colored dots on left indicate the locations of the correspondingly-colored diurnal curves on the right.